

## Prospects for Steady-State Scenarios on JET

X. Litaudon<sup>1</sup>, J.P.S. Bizarro<sup>2</sup>, C.D. Challis<sup>3</sup>, F. Crisanti<sup>4</sup>, P.C. De Vries<sup>3</sup>, P. Lomas<sup>3</sup>, F.G. Rimini<sup>1</sup>, T.J.J Tala<sup>5</sup>, R. Akers<sup>3</sup>, Y. Andrew<sup>3</sup>, G. Arnoux<sup>1</sup>, J.F Artaud<sup>1</sup>, Yu F. Baranov<sup>3</sup>, M. Beurskens<sup>3</sup>, M. Brix<sup>3</sup>, R. Cesario<sup>4</sup>, E. De La Luna<sup>6</sup>, W. Fundamenski<sup>3</sup>, C. Giroud<sup>3</sup>, N.C. Hawkes<sup>3</sup>, A. Huber<sup>7</sup>, E. Joffrin<sup>3</sup>, R.A Pitts<sup>8</sup>, E. Rachlew<sup>9</sup>, S.D.A Reyes-Cortes<sup>2</sup>, S. Sharapov<sup>3</sup>, O. Zimmermann<sup>7</sup> and the JET EFDA contributors\*

<sup>1</sup>Association Euratom-CEA, CEA/DSM/DRFC-Cadarache 13108, S<sup>t</sup> Paul Durance, France

<sup>2</sup>Centro de Fusão Nuclear, Associação Euratom-IST, Instituto Superior Técnico, 1049-001 Lisboa, Portugal

<sup>3</sup>Association Euratom-UKAEA, Culham Science Centre OX14 3DB Abingdon, OXON UK

<sup>4</sup>Associazione Euratom-ENEA, ENEA Centro Ricerche Frascati C.P. 65, 00044 Italy

<sup>5</sup>Association Euratom-TEKES, VTT, P.O. Box 1000, FIN-02044 VTT, Finland

<sup>6</sup>Asociacion Euratom-CIEMAT, ES Avenida Complutense 22 E-28040 Madrid Spain

<sup>7</sup>Assoziationen Euratom-Forschungszentrum, Jülich D- 52425 Jülich Germany

<sup>8</sup>Association Euratom-Confédération Suisse CRPP EPFL 1015 Lausanne Switzerland

<sup>9</sup>Association Euratom-VR, Dept Phys., KTH, SE 10691, Stockholm Sweden

e-mail contact of first author: [xavier.litaudon@cea.fr](mailto:xavier.litaudon@cea.fr)

**Abstract.** In the 2006 experimental campaign, progress has been made to operate non-inductive scenarios at higher applied powers (27MW) and density ( $n_i \sim 4 \times 10^{19} \text{m}^{-3}$ ), with ITER-relevant safety factor ( $q_{95} \sim 5$ ) and plasma shaping, taking advantage of the new divertor capabilities. The extrapolation of the performance using transport modelling benchmarked on the experimental database indicates that the foreseen power upgrade ( $\sim 45\text{MW}$ ) will allow the development of non-inductive scenarios where the bootstrap current is maximised together with the fusion yield and not, as in present day experiments, at its expense. The tools for the long-term JET programme are the new ITER-like ICRH antenna ( $\sim 15\text{MW}$ ), an upgrade of the NB power (35MW/20s or 17.5MW/40s), a new ITER-like first wall, a new pellet injector for ELM control together with improved diagnostic and control capability. Operation with the new wall will set new constraints on non-inductive scenarios that are already addressed experimentally and in the modelling. The fusion performance and driven current that could be reached at high density and power have been estimated using either 0-Dimensional or 1-1/2D validated transport models. In the high power case (45MW), the calculations indicate the potential for the operational space of the non-inductive regime to be extended in terms of current ( $\sim 2.5\text{MA}$ ) and density ( $n_i > 5 \times 10^{19} \text{m}^{-3}$ ), with high  $\beta_N$  ( $\beta_N > 3.0$ ) and a fraction of the bootstrap current within 60-70% at high toroidal field ( $\sim 3.5\text{T}$ ).

### 1. Introduction

Improvement of the tokamak concept in terms of high confinement and stability without the need for large plasma current is a crucial challenge that could ultimately lead to the operation of future devices in continuous mode. These challenging “advanced tokamak” (AT) scenarios (high  $\beta_N$  operation) could lead to more efficient electricity production in a reactor. They are foreseen to fulfil the second of the ITER objectives, namely “to aim at demonstrating steady state operation using non-inductive current drive with a fusion gain  $Q \geq 5$ ”. This advanced mode of operation is far less mature than the inductive ELMy H-mode and is known to be sensitive to plasma profiles such as the pressure, current density and rotation. Therefore, the development of this scenario on ITER is likely to be demanding in terms of control requirements and operating time. In view of preparing reliable ITER AT operation, effort and progress have been continuously made on JET to achieve plasma regimes suitable for steady state tokamak operations, i.e. where a large fraction of the plasma current is non-inductively driven [1-4].

\*See Appendix of M.L. Watkins et al., Fusion Energy 2006 (Proc. 21<sup>st</sup> Int. Conf. Chengdu, 2006) IAEA, (2006)

The critical physics issues, relevant to a reliable extrapolation of AT regimes to next step experiments such as ITER, that need to be addressed in present-day experiments or modelling activities, have been recently reviewed [5]. Among the five critical issues that have been discussed in [5], the JET programme could particularly contribute to address the compatibility of core with edge transport barrier for achieving high confinement required for steady-state operation, while respecting constraints imposed by the plasma facing components. In this context, a new beryllium wall in the main chamber and a tungsten divertor will be installed on JET. It should be stressed that the edge conditions of the non-inductive regimes on JET are usually characterised by a high edge temperature and low density but at ITER-relevant collisionality. Operation with the new ITER-like wall at high power and during long duration will set new constraints on non-inductive scenarios: e.g. higher density, different edge radiation level without carbon, compatibility of high core confinement with the new power handling and plasma exhaust capabilities. Some of these aspects need already to be addressed in the present (2006) and coming experimental campaign prior to the new wall installation. New AT scenarios need to be prepared both experimentally and with transport modelling imposing this new set of constraints. Fully non-inductive operation, in particular at high density, will require an extension of the heating, current drive and fuelling capability of the JET device. Therefore, in addition to the installation of new plasma facing components, the tools for the long-term JET programme in preparation of ITER operation is the ITER-like ion cyclotron resonance heating, ICRH, antenna (power up to  $\sim 15$  MW), an upgrade of the neutral beam (NB) power (35 MW/20s or 17.5 MW/40s), a new pellet injector for edge localised mode, ELM, control together with improved diagnostic and control capability.

The AT programme on JET for the present experimental campaign has been prepared keeping this long-term objective in mind. The approach that has been adopted is to address the various critical issues separately during the 2006 and the coming campaigns, with a view to full scenario integration when the future JET upgrades are complete. To form and sustain reliable non-inductive scenarios as close as possible to ITER relevant non-dimensional parameters, the JET AT programme aims to develop and exploit advanced regimes separately:

- (i) at ITER-relevant safety factor and plasma shaping (high triangularity) taking advantage of the new divertor capabilities;
- (ii) at high values of pressure normalized to plasma current and magnetic field (beta) to investigate MHD stability limits and optimize the bootstrap current;
- (iii) where temperature and q-profiles are simultaneously controlled in real-time with advanced algorithms that include the two different time scales for heat and current diffusion;
- (iv) with edge conditions appropriate for future modifications to the plasma facing components (ITER-like wall project) and for ITER advanced regimes.

In the first part of this paper (section 2), the progress made essentially on point (i) and (iv) is first reviewed. Then, in section 3 and 4, we will show how the present results extrapolate at higher power and density in conditions imposed by the future ITER-like wall. To estimate the fusion performance and the non-dimensional parameters that could be reached at high density and power, a simplified 0-D model has been developed based on global scaling for the energy confinement time and the current drive efficiencies. Non-inductive mechanisms considered were lower hybrid current drive, LHCD, neutral beam current drive, NBCD and the bootstrap current. The extension of the full current drive operating space in terms of plasma current, density, bootstrap current fraction and fusion performance is quantified in section 3. The simplified 0-D approach, which allows the operating space to be identified, is complemented in section 4, before the conclusion (section 5), with more sophisticated modelling of the full time-dependent scenario with the complete suite of heating and current drive models (JETTO, CRONOS).

## 2. Development of non-inductive current drive scenarios at ITER triangularity

In past experimental campaigns, development of highly non-inductive current drive regimes was mainly carried out with plasma shapes at moderate triangularity values,  $\delta \sim 0.25$  [1,3,6] where mild ELM activity (type III) could be combined with an internal transport barrier, ITB [4]. In these regimes, the ITB strength and the radial q-profiles have been controlled on a duration approaching the resistive time using real time algorithms [6-8]. Attempts to develop ITB regimes at higher triangularity in the years 2000-2002, with the Mark-2 Gas-Box divertor equipped with a septum, lead to the conclusion that the large edge MHD effects (Type I ELMs) were dominant and prevented the sustainment of ITBs for quasi-steady-state operation [9]. During the experimental campaign 2002-2004, an effort was made to mitigate the ELMs by injecting deuterium and/or neon gas. This successfully showed that long lasting, wide ITBs could be sustained during 2.5s at  $\delta = 0.45$  (averaged between upper  $\delta_u$  and lower  $\delta_l$  triangularity at the separatrix),  $q_{95} = 7.5$  and 1.5MA/3.45T (#62293) [2]. The configurations (in particular  $\delta_l \leq 0.4$ ) were limited with the restriction on the position of the strike points originating from the lack of power handling on the septum replacement plates. During the 2004-2005 shutdown, the installation of a new load-bearing septum replacement plate (LB-SRP) in the divertor offers more freedom in the choice of configurations and provides access to higher triangularity ( $\delta_l$  up to 0.55) at higher plasma current.

One of the first objectives of the AT research on JET during the 2006 experimental campaign was to fully exploit these upgraded divertor capabilities offered by the newly installed septum plates. During the high power heating phase, two new configurations were successfully developed (Fig. 1 (left)) with either (i) simultaneously high values of upper and lower triangularities ( $\delta_u \leq 0.45$ ,  $\delta_l \leq 0.55$ , this configuration being called ITER-AT) or, alternatively, (ii) keeping an ITER value of lower triangularity while having a moderate upper triangularity ( $\delta_u \leq 0.2$ ,  $\delta_l \leq 0.55$ , this configuration being called LUD for Lower Upper Delta). In addition, effort has been made to develop an early transition towards the LUD or ITER-AT configurations during the current ramp-up phase (low power prelude phase used to shape the target q-profile prior to the application of the full heating power). This early transition towards highly shaped plasmas prevents variations in the configurations (and related plasma volumes, magnetic axis, internal inductance etc) during the main heating phase, where such changes are expected to affect the pre-shaped target q-profile and its evolution. Two different target q-profiles were reached at the end of the prelude phase applying either (i) LHCD (2MW) during a moderate current ramp-up phase (typically at 0.3MA/s) to form a deeply reversed q-profile having the characteristics of a current hole with an associated early electron ITB or (ii) on-axis ICRH electron heating with a fast current rise (up to 0.6MA/s) to form a weakly reversed current profile with a broad region of zero or weakly negative magnetic shear. The plasma current in the current flat top ( $I_p \sim 1.9$ MA) and the on-axis toroidal magnetic field ( $B_0 \sim 3.1$ T) have been selected to have a  $q_{95}$ -value (at 95% of the poloidal flux,  $q_{95}$ ) close to five as prescribed for ITER steady-state regimes.

Even if these configurations and target q-profiles have not yet been fully exploited to reach their performance potential, the results obtained so far are encouraging and are summarized in Fig. 1 (right) where the stored diamagnetic energy values are plotted versus the total applied power. The configuration that has been mostly exploited so far is the LUD with up to 27MW of applied power comprising of 20MW of NBI, 5MW of ICRH and 2MW of LHCD powers in the main heating phase (the time evolution of the main parameters of an example discharge, #66498, is shown in Fig. 2 (left)). The most striking difference between the low and high  $\delta$  discharges is that the high  $\delta$  configurations allow the development of ITB regimes at simultaneously higher edge ( $n_{ped} \sim 2.5 \times 10^{19} \text{m}^{-3}$ ) and core density ( $n_{eo} \sim 6 \times 10^{19} \text{m}^{-3}$ ), leading to a line averaged density ranging between  $3.6\text{-}4 \times 10^{19} \text{m}^{-3}$  and with ion temperatures,  $T_i$ , closer to

that of the electrons,  $T_e$  ( $T_{i0} \sim 8\text{-}10\text{keV}$ ,  $T_{e0} \sim 7\text{-}8\text{keV}$  where  $T_{i0}$  &  $T_{e0}$  are the central  $T_i$  and  $T_e$  values) at a toroidal rotation up to  $V_{\text{tor}} \sim 300\text{km/s}$ . The core transport barrier is typically at mid-radius and appears clearly on the ion temperature, toroidal rotation and density profiles (Fig. 2 (right)). These ITBs profiles are combined with high frequency type I ELMs ( $f \sim 100\text{-}80\text{Hz}$ ) at relatively high density at the top of the pedestal  $n_{\text{eped}} \sim 2.5\text{-}2.8 \times 10^{19}\text{m}^{-3}$  with  $T_{\text{eped}} \sim 1.1\text{-}1.3\text{keV}$ . Compared to the previously moderate triangularity regimes where the H-mode pedestal parameters were typically  $T_{\text{eped}} \sim 2\text{-}3\text{keV}$  at  $n_{\text{eped}} \sim 1.5 \times 10^{19}\text{m}^{-3}$  (type III-ELMs) [10], these new configurations are promising in terms of their future application with the new ITER-like wall. The proximity of the inner strike point to the divertor tile at the top of the divertor leads to the formation of a highly localized radiation pattern close to the X-point that may reduce the performance of the edge transport barrier. Investigation of the role of the X-position relative to the inner divertor tiles is part of the future optimization of the configuration. The current-hole profile at the start of the main heating phase evolves towards weakly reversed  $q$ -profile when the density is increased with typically  $q_{\text{min}} \sim 2$  (at  $r/a \sim 0.3$ ) and  $q_0 \leq 5$ . EFIT equilibrium calculations constrained by MSE data as well as the observation of Alfvén cascades when  $q_{\text{min}}$  crosses a rational  $q$ -surface at the start and the end of the high power phase, both lead to the conclusion that the  $q$ -profile keeps a non-monotonic shape during the main heating phase that lasts 4s. TRANSP interpretative simulations indicate that the bootstrap current reaches up to  $0.7\text{MA}$  at  $\beta_N \sim 1.8$ , while the NB and LH currents are, respectively, at a level  $0.3\text{MA}$  and  $0.25\text{MA}$ , leading to a non-inductive fraction of up to 70% at the peak of the performance.

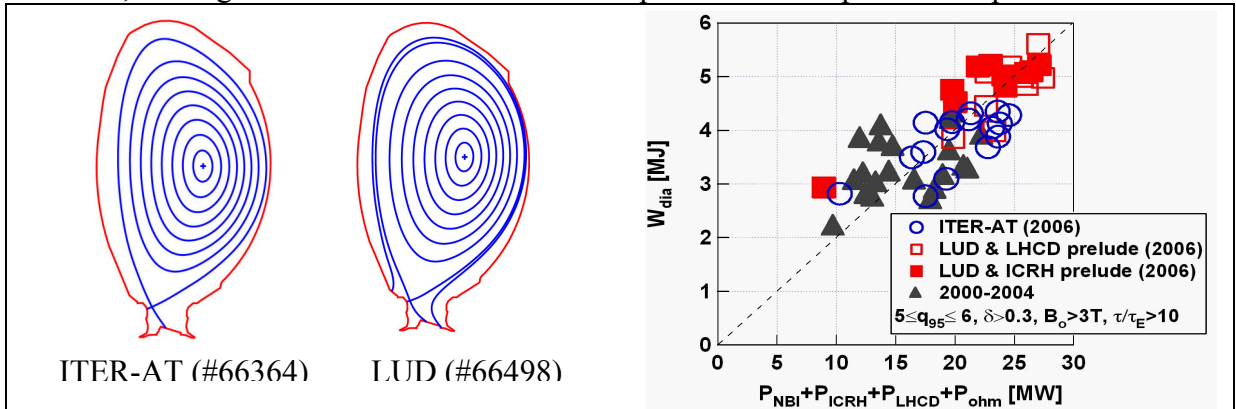


**Fig. 1:** (left) ITER-AT & LUD magnetic configurations developed in 2006. (right) Diamagnetic energy versus the applied power in the main heating phase for ITER-AT and LUD configurations with either a current-hole (LHCD prelude) or a weakly reversed shear (ICRH prelude) target  $q$ -profiles. The 2000-2004 high  $\delta$ -data are shown for comparison. Data selected at  $5 \leq q_{95} \leq 6$ ,  $\delta > 0.3$ ,  $B_o > 3\text{T}$ ,  $\tau/\tau_E > 10$  where  $\tau$  is the duration of high performance phase and  $\tau_E$  the energy confinement time.

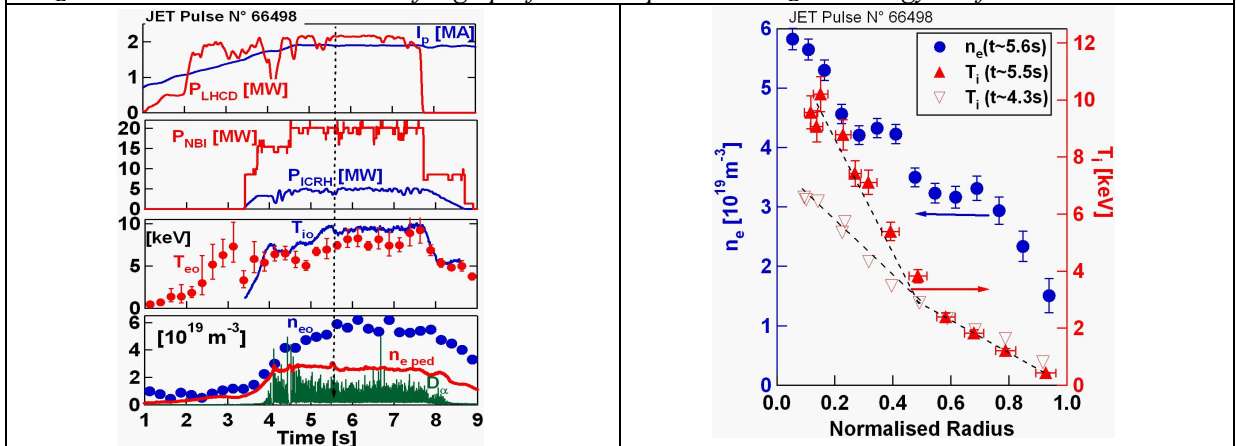


**Fig. 2:** (left) Time evolution of the main parameters for discharge #66498 with a LUD magnetic configuration (LHCD in the prelude phase). (right) Electron density  $n_e$  (Thomson scattering) and ion temperature profile  $T_i$  (CXs) at the time where the neutron rate reaches its maximum value ( $t \sim 5.5\text{s}$ ). Reference  $T_i$  profile prior to the ITB formation is also shown.

### 3. Operational domain for fully non-inductive current drive regimes

By increasing the heating power and current drive capability, the operational space of fully non-inductive regimes could be dramatically extended and could be made compatible with the divertor and beryllium wall (e.g. high edge density and low edge temperature). The heating power is required for increasing beta and the bootstrap current fraction, the remainder being driven by externally applied current drive. In the proposed operational diagram for non-inductive current drive, the plasma current,  $I_p$ , is plotted against the line-averaged density,  $n_l$ , at various power levels (Fig. 3). The plasma current is entirely driven by non-inductive means and is the sum of the LH, NB and bootstrap currents as deduced from a 0-D model that fits the present JET AT database. The bootstrap current is assumed to scale as  $C_{bs}(a/R)^{1/2}\beta_p \propto q_{95}\beta_N$  (with  $C_{bs}=0.3$ ). The LHCD and NBCD efficiencies are also deduced from the current drive, CD, values achieved in highly non-inductive CD regimes, yielding the normalised CD efficiencies ( $\eta_{CD} = n_l R I_{CD} / P_{CD}$ )  $\eta_{LHCD} = 1.6 \times 10^{19} \text{ m}^{-2} \text{ A/W}$  and  $\eta_{NBCD} = 0.16 \times 10^{19} \text{ m}^{-2} \text{ A/W}$ . Optimising the full CD performance requires the heating power and the confinement quality to be increased simultaneously. In the calculation it is assumed that confinement scales as the ELMy H-mode [11], but with a confinement enhancement factor increasing with power up to  $H_{IPB98(y,2)} \sim 1.5$  at 45MW. This trend is observed in the JET database in plasmas with ITBs (c.f. insert in Fig. 4), when wide ITBs that enclose a large volume with improved confinement have been formed at power levels up to 25MW with  $H_{IPB98(y,2)} \sim 1.5$  ( $H_{ITER-89P} \sim 3$ ) in the moderate triangularity configuration. The  $H_{IPB98(y,2)}$ -factor for improved confinement is the free parameter in these calculations and is unknown (c.f. next section for transport simulation). This factor will affect directly the bootstrap current fraction and the total plasma current. The diagram shown on Fig. 3 indicates two operational regimes:

- (i) at low bootstrap current fraction,  $I_{boot}/I_p$  ( $<50\%$ ) and low  $\beta_N$  ( $<2$ ), where  $I_p$  decreases rapidly with increasing density since the current is mainly driven by external means;
- (ii) at high  $I_{boot}/I_p$  ( $>50\%$ ), high  $\beta_N$  and high power ( $>30\text{MW}$ ) where high density full CD operation is feasible. The plasma current is practically independent of density since the decrease of the externally driven current with density is compensated by an increase of the bootstrap current with  $\beta_N$  (that raises with density through the confinement scaling law).

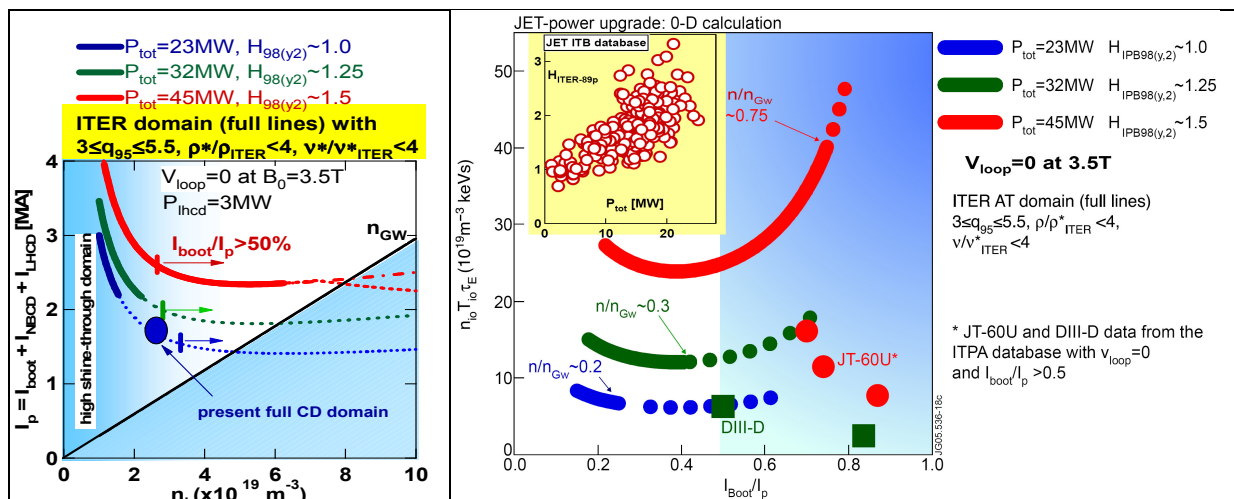


**Fig. 3:** JET fully non-inductive domain of plasma current versus density at  $B_o=3.5T$  for various power levels and confinement factors. For MHD considerations,  $\beta_N$  is limited to 3.5

**Fig. 4:** Triple fusion product ( $n_{l0} T_{10} \tau_E$ ) versus  $I_{boot}/I_p$  at  $V_{loop}=0$  for various power levels. Experimental points from JT-60U & DIII-D (2005 ITPA ITB database) with  $V_{loop}=0$  and  $I_{boot}/I_p > 50\%$  (no JET data presently meets these two conditions simultaneously). **Insert:**  $H_{ITER-89P}$  versus total power (JET ITB database at  $B_o \sim 3.45T$ ,  $4.5 \leq q_{95} \leq 6.5$ ,  $\delta \sim 0.2$ ,  $2 \leq n_l \leq 4 \times 10^{19} \text{ m}^{-3}$ )

The operational domain, calculated at  $B_0=3.5\text{T}$ , is limited by a low density region, where shine-through is expected to be high, and by a high density boundary at the Greenwald density. The thick line corresponds to conditions where simultaneously  $3 \leq q_{95} \leq 5.5$ ,  $\rho/\rho^*_{\text{ITER}} < 2.2$  and  $v/v^*_{\text{ITER}} < 4$ , that is approaching the ITER-relevant parameter space.

Advanced tokamak operation at a power level above 32MW is required to ensure stationary conditions at relevant densities and q-profile with  $q_{95} \sim 5$  at  $B_0=3.5\text{T}$ . With 32MW, fully non-inductive AT regimes at  $q_{95}=5$  (and  $B_0=3.5\text{T}$ ) will be limited to low density ( $n_i < 4 \times 10^{19} \text{m}^{-3}$ ) and low current (below 2.0MA). A power level of 45MW (assuming  $H_{\text{IPB98}(y,2)} \sim 1.5$ ) gives access to regime (ii) where, as in a future steady-state reactor, the bootstrap current is maximised together with the fusion yield and not at the expense of the latter as in present-day experiments, i.e. by lowering  $I_p$  and/or toroidal field. This is illustrated in Fig. 4, where the calculated fusion triple product is plotted against  $I_{\text{boot}}/I_p$  for various power levels. In the high power case, the calculations indicate that the operational space of the non-inductive regime is extended in terms of current ( $\sim 2.5\text{MA}$ ) and density ( $n_i > 5 \times 10^{19} \text{m}^{-3}$ ) with high  $\beta_N$  ( $\beta_N > 3.0$ ) together with  $I_{\text{boot}}/I_p$  in the range of 70% at high toroidal field ( $\sim 3.5\text{T}$ ).

#### 4. Transport simulations of bootstrap dominated regime with the power upgrades

The approach described in section 3, that allows the operating space to be identified, is complemented with more sophisticated transport modeling of the time-dependent scenario with the complete suite of heating and current drive models (CRONOS and JETTO).

Firstly, the simplified version of the CRONOS code has been used (1/2-D) that solves the heat and current diffusion equations with simplified 0-D models for the non-inductive sources and with simple radial dependence of the transport coefficients ensuring that the integrated energy content is in agreement with the global thermal confinement scaling laws (the line averaged density and the density profile peaking are given as input) [12]. The agreement between the simulated global performance and the measurements for the discharge #66498 shown in Fig. 5 (left) is obtained with the confinement factor  $H_{\text{IPB98}(y,2)} \sim 0.8$ . The bootstrap current (0.65MA) and total non-inductive current one (up to 1.15MA) are in fair agreement with the TRANSP interpretative simulations. The performance predictions are illustrated in Fig. 5 (right) for an increase of the applied power up to 45MW ( $B_0=3.5\text{T}$ ) with  $H_{\text{IPB98}(y,2)} \sim 1.5$  while prescribing a constant flux operation at  $t=10\text{s}$ . These simulations confirm that bootstrap-dominated regimes can be reached at this power level provided that good confinement can be sustained.

Secondly, a full set of predictive transport simulations have been performed with the JETTO code using the empirical Bohm/gyro-Bohm model together with the experimental criterion for the ITB triggering based on a combination of magnetic and ExB shear [13-14]. The five transport equations are solved simultaneously, i.e. ion and electron heat transport, particle transport, toroidal momentum transport and current diffusion. The simulations yield predictions for  $T_i$ ,  $T_e$ ,  $n_e$ ,  $v_{\text{tor}}$  and  $q$ , respectively. The Prandtl number, defined as the ratio between momentum and ion heat diffusivity, is set to 0.3 in agreement with recent studies on JET [15]. Fig. 6 (left) shows the simulated profiles together with their experimental counterparts (#66498). The results confirm that the core turbulence reduction via the combined role of ExB and magnetic shear effects is necessary to reproduce the core performance.

Keeping the same assumptions for the transport models, JETTO predictive simulations of  $T_i$ ,  $T_e$ ,  $n_e$ ,  $v_{\text{tor}}$ ,  $q$  and non-inductive sources have been performed for the 45MW JET power upgrade case. The uncertainties in the predicted performance depend not only on the models for core transport and non-inductive sources, but also on the assumptions made for the boundary conditions taken at the top of the H-mode pedestal. The approach that has been adopted to choose the pedestal parameters was to adjust them so that in the simulations without ITB, the global thermal confinement properties follow the IPB-98(y,2) scaling [11]

$H_{IPB98(y,2)} \sim 1.0$ . The pedestal density is fixed at  $n_{eped} = 2.5 \times 10^{19} \text{ m}^{-3}$  while the temperatures at the pedestal are estimated at  $T_{iped} = 1.8 \text{ keV}$ ,  $T_{eped} = 1.5 \text{ keV}$ . The pedestal energy content is consistent with the lower value (within the error bar of the scaling) of the predicted one using the 0-D scaling proposed in [16] that best fits the ELMy-H mode ITPA database. Figure 6 (right) shows the thermal profiles when a wide ITB is triggered with the off-axis LHCD power deposition and the formation of a low magnetic shear region at  $\rho \sim 0.7$ . The thermal energy content reaches 11MJ ( $H_{IPB98(y,2)} \sim 1.5$ ), leading to  $I_{boot}/I_p \sim 75\%$  at  $n_i \sim 5.5 \times 10^{19} \text{ m}^{-3}$  ( $n_i/n_{GW} \sim 0.7$ ) and a core toroidal rotation of  $\sim 360 \text{ km/s}$ . A key ingredient to sustain the low magnetic shear region and the ITB is the amount of off-axis current driven by LHCD. By reducing from 3MW down to 2MW the LHCD power level, it is found that ITB could not be sustained at these densities. Even at  $P_{LHCD} \sim 3 \text{ MW}$ , simulations indicate that relaxation oscillations of confinement between two thermal states (an ITB and a non-ITB state) could occur as observed in the high bootstrap experiments on DIII-D [17] or with LHCD alone on Tore Supra [18]. In the modelling an increase of LH power above 3MW is required to maintain the plasma in the high core thermal confinement state without relaxation.

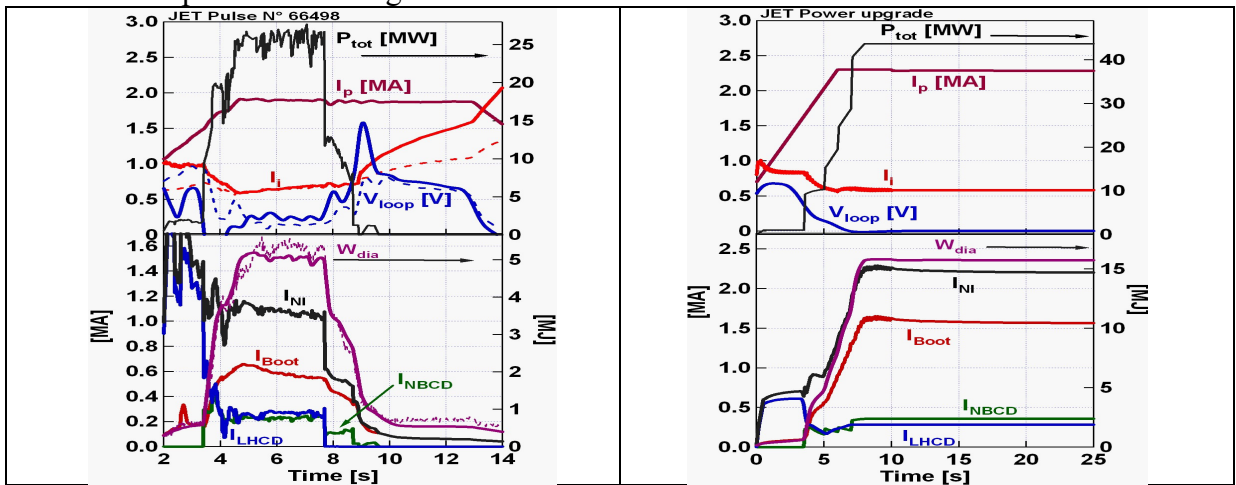


**Fig. 5:** CRONOS 1/2-D simulations: (left) JET pulse #66498. Time evolution of  $P_{tot}$ ,  $I_p$ , internal inductance  $l_i$ , loop voltage  $V_{loop}$  and total energy content  $W_{dia}$ , bootstrap current  $I_{boot}$ ,  $I_{LHCD}$ ,  $I_{NBCD}$  and the non-inductive current. The dashed lines correspond to the experimental values of  $l_i$ ,  $V_{loop}$  &  $W_{dia}$ ; (right) Non-inductive CD performance at  $P_{tot} = 45 \text{ MW}/20 \text{ s}$  ( $P_{LHCD} = 3 \text{ MW} + P_{ICRH} = 10 \text{ MW} + P_{NBI} = 32 \text{ MW}$ ).

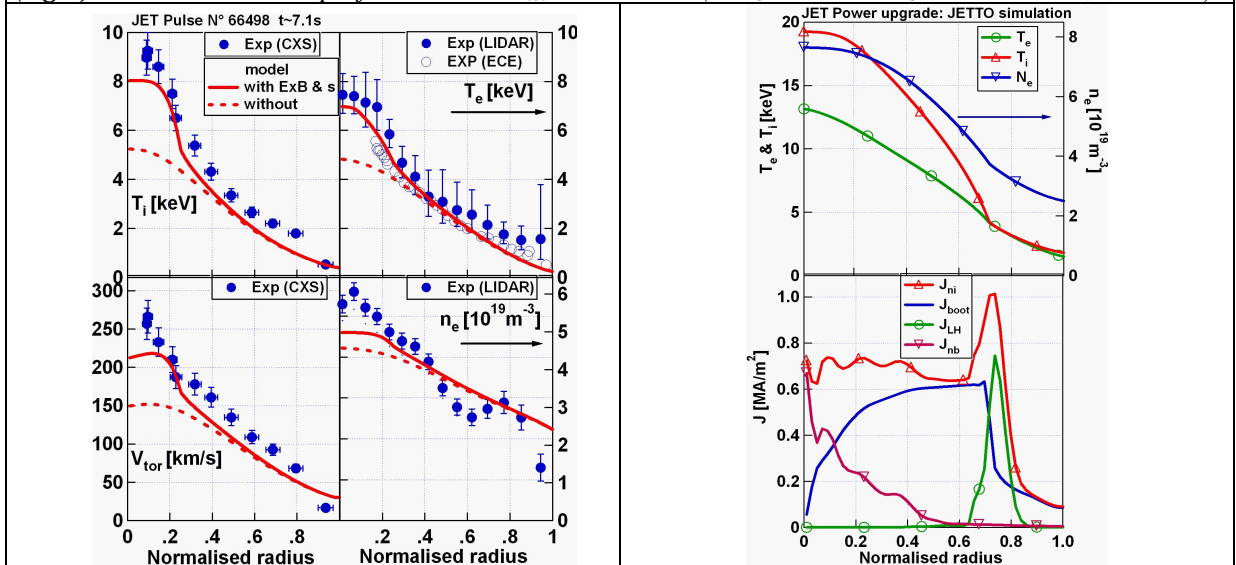


**Fig. 6:** JETTO simulations: (left) Experimental (closed symbols) and simulated  $T_i$ ,  $T_e$ ,  $n_e$  and  $V_{tor}$  profiles of the JET pulse #66498 using the Bohm/Gyro-Bohm model with either the combined ExB and magnetic shear stabilization effects for the ITB formation (full line) or without (dashed line); (right) Simulated  $T_i$ ,  $T_e$ ,  $n_e$  and non-inductive current profiles of the fully non-inductive performance exploiting the JET power upgrade at  $P_{tot} = 45 \text{ MW}$  ( $P_{LHCD} = 3 \text{ MW} + P_{ICRH} = 10 \text{ MW} + P_{NBI} = 32 \text{ MW}$ )

## 5. Conclusion

Experimental effort is being made to develop AT scenarios on JET by exploiting the capability that is offered by the heating/CD systems and the new divertor. Non-inductive regimes with ITBs have been developed at  $q_{95} \sim 5$  ( $I_p \sim 1.9\text{MA}$ ,  $B_0 \sim 3.1\text{T}$ ) closer to the ITER shape with high value of triangularity ( $\delta_u \leq 0.45$ ,  $\delta_l \leq 0.55$ ) by applying up to 27MW of additional heating power (20MW of NBI, 5MW of ICRH and 2MW of LHCD). An ongoing effort is also devoted to define AT scenarios that could be made compatible with the constraints that will be imposed by the upgraded plasma facing components on JET, i.e. the ITER-like wall project. In this context, the AT scenarios at high  $\delta$  offer the opportunity to increase the edge density pedestal ( $n_{ped} \sim 2.5 \times 10^{19} \text{m}^{-3}$ ) and the core density while keeping mild high frequency ELMs with reduced values of edge temperature. At peak performance the non-inductive current fraction reaches 70% of the total plasma current. Operation at lower toroidal field ( $\sim 2\text{T}$ ) and current ( $\sim 1.5\text{MA}$ ) is foreseen in the 2006/2007 experimental campaign to increase the normalized performance and bootstrap current fraction with the available power.

At high field operation, an upgrade of the heating and CD power is required to operate JET in fully non-inductive conditions at high density to be compatible with the divertor and beryllium wall. The extension of the operational space of non-inductive regimes by increasing the additional power has been quantified using 0-D and 1-1/2D transport simulations validated using JET data. Core confinement enhancement is a key issue when predicting the expected performance. In the high power case (45MW), the operational space of the non-inductive regime is extended in terms of current ( $\sim 2.5\text{MA}$ ), density ( $n_i > 5 \times 10^{19} \text{m}^{-3}$ ) at high  $\beta_N$  ( $\beta_N > 3.0$ ) together with  $I_{Boot}/I_p$  in the range of 60-70% at high toroidal field ( $\sim 3.5\text{T}$ ). This opens the opportunity to explore the  $\beta$ -dependence of core confinement if a MHD stable route is found. These performance could be reached if a confinement enhancement factor of up to  $H_{IPB98(y,2)} \sim 1.5$  is sustained at 45MW. The 1-1/2D transport simulations indicate that wide ITB could be formed and sustained in the low magnetic shear region maintained by off-axis LHCD and bootstrap current in order to provide the required core confinement enhancement. A level of LHCD power of 3MW could be marginal to sustain bootstrap dominated regimes. Indeed, cyclic relaxation of the fusion performance has been observed numerically and is linked to the coupled evolution of pressure (ITB) and q-profiles. An increase of LHCD coupled power above 3MW could contribute to sustain the fusion performance by avoiding the thermal relaxations and by keeping a low magnetic shear at large radius.

## References

- [1] Tuccillo A.A., Crisanti F., Litaudon X. et al Nucl. Fusion **46** (2006) 214–224
- [2] Rimini F.G. et al Nucl. Fusion **45** (2005) 1481
- [3] Litaudon X., Bécoulet A., Crisanti F. et al Nucl. Fusion **43** (2003) 565
- [4] Challis C.D. Plasma Phys. Control. Fusion **46** (2004) B23
- [5] Litaudon X. Plasma Phys. Control. Fusion **48** (2005) A1
- [6] Mazon D. et al 2002 Plasma Phys Control Fusion **44** (2002) 1087
- [7] Laborde L. et al 2005 Plasma Phys Control Fusion **47** (2004) 155
- [8] Moreau D. et al 2006 this conference
- [9] Crisanti F. et al Plasma Phys. Control. Fusion **45** (2003) 379
- [10] Sarazin Y. et al Plasma Phys. Control. Fusion **44** (2002) 2445
- [11] ITER Physics Basis Nucl. Fus Vol. **39** (1999) 2175
- [12] Basiuk V. et al Nucl. Fusion **43** (2003) 822
- [13] Tala T.J.J. et al Plasma Phys. Control. Fusion **43** (2001) 507
- [14] Tala T.J.J. et al Nucl. Fusion **45** (2006) 548
- [15] De Vries P.C. et al to appear in Plasma Phys. Control. Fusion (2006)
- [16] Cordey J.G. et al Nucl. Fusion **43** (2003) 670
- [17] Politzer P.A. et al Nucl. Fusion **43** (2005) 417
- [18] Giruzzi G. et al Phys. Rev. Lett. **91** (2003) 135001-1